Single-Crystal Multifrequency EPR Evidence for a Quasi-Low-Dimensional Spin Exchange in 3-*n*-Butyl-2,4,6-Triphenylverdazyl

N. S. Dalal,*,† Alex I. Smirnov,*,‡ Tatyana I. Smirnova,§ R. L. Belford,⊥ A. R. Katritzky,|| and S. A. Belyakov*,||

Chemistry Department and National High Magnetic Field Laboratory, Florida State University, Tallahassee, Florida 32306, Illinois EPR Research Center, College of Medicine and Veterinary Medicine and Department of Chemistry, University of Illinois at Urbana−Champaign, Urbana, Illinois 61801, and Department of Chemistry, University of Florida, Gainesville, Florida 32611

Received: September 15, 1997[⊗]

Verdazyls, 1,2,3,4-tetrahydro-*s*-tetrazin-1-(2*H*-yls), are a series of stable organic free radicals some of which in solid form exhibit ferromagnetism and spin-Peierls transitions. Molecular mechanisms responsible for these properties remain somewhat unclear. This study reports on the growth of single crystals of several substituted verdazyls and multifrequency (1.4−94.3 GHz) EPR measurements on single crystals of 3-*n*-butyl-2,4,6-triphenylverdazyl, a model compound in the series. The angular, temperature, and magnetic field dependence of the EPR line width and the temperature dependence of the *g*-factor anisotropy provide direct evidence of a pseudo-low-dimensional spin diffusion in the crystal lattice. Analysis of the EPR line width for the crystal, oriented with the *c*-axis at the magic angle, $\theta \approx 54.7°$ with respect to the external magnetic field, indicates a weak logarithmic dependence upon the frequency of the EPR experiment typical for a quasi-two-dimensional spin system.

Introduction

The synthesis and characterization of novel magnetic and electrooptic organic materials is a topic of current research activity.[1,2] Two strategies have been employed for developing organic magnets: (i) preparation of solids with unpaired electrons in orthogonal orbitals, such as polycarbenes[1−3] and nitrenes;[4] and (ii) synthesis of solids based on free radical moieties.[5−7] Both strategies have been partially successful.[1,2] In the free-radical approach, one area of interest is the synthesis and characterization of free-radical-based solids that exhibit highly anisotropic, i.e., low-dimensional, magnetic properties. The verdazyl (1,2,3,4-tetrahydro-*s*-tetrazin-1-(2*H*-yls)) series of highly stable organic free radicals is one class of such compounds. Recently, several new substituted verdazyls have been synthesized and examined with magnetic dc and ac susceptibility over a broad range of magnetic field and temperatures.[7−13] Variable-temperature susceptibility data (T < 100 K) for 3-(4-cyanophenyl)-1,5-dimethyl-6-oxoverdazyl radical can be satisfactorily explained by a one-dimensional antiferromagnetic Heisenberg alternating chain model with a spin-Peierls transition at around 15 K.[10] Another substituted verdazyl, 3-(4-chlorophenyl)-1,5-dimethyl-6-thioxoverdazyl, was found to show an anomalous magnetization of ferromagnetic nature just below the critical temperature $T_c = 0.71$ K.[11]

Despite some progress in characterization and understanding the magnetic behavior of the verdazyls,[7−19] a detailed microscopic mechanism underlying the observed effects has not yet appeared. As has been pointed out in several recent studies of these compounds, one possible factor hampering further progress appears to be the lack of single crystals of suitable quality.[11−14,17,18] The present study was undertaken to explore whether a recently synthesized class of verdazyls can be grown as millimeter-size single crystals. Such single crystals can be suitable not only for EPR but also for detailed magnetic, thermodynamic, and spectroscopic investigations.

Our second objective was to explore the potential of electron paramagnetic resonance (EPR) spectroscopy as a sensitive and direct method to investigate the possible low-dimensional behavior of spin−spin interactions in verdazyls. Usually, the low-dimensional character of a magnetic solid is observed as a broad maximum in a plot of the static (dc) magnetic susceptibility vs temperature. The temperature, T_{max}, at which the maximum susceptibility occurs can characterize low-dimensional magnetic interactions; the higher the value of T_{max}, the stronger the low-dimensional magnetic interaction.[19] However, dc magnetic susceptibility, being a static property, cannot yield any direct information on the spin dynamics. On the other hand, as has been already shown, EPR can indeed serve as a sensitive tool in probing the spin correlations in low-dimensional magnetic systems.[20−26] For example, the low dimensionality in a spin system can be recognized from the angular dependence of the peak-to-peak line width, ΔB_{p-p}, which for a low-dimensional system is:[23,24,26]

$$\Delta B_{p-p} \approx |3 \cos^2 \theta - 1|^n \qquad (1)$$

where θ is the angle between the direction of the magnetic field and the chain axis and n depends on the model and dimensionality (e.g., $n = 4/3$ for a one-dimensional model[27]). This dependence is in contrast to the three-dimensional case, where the line width is proportional to $(1 + \cos^2 \theta)$.[28] In addition, the frequency dependence of the EPR line width at a special (magic angle) crystal orientation with respect to the applied Zeeman magnetic field can be used to determine the effective dimensionality of the spin diffusion process and to evaluate the spin diffusion constant.[21,26]

* Address for correspondence: Naresh Dalal, Department of Chemistry, Florida State University, Tallahassee, FL 32306-4390; Tel. (904)-644-3398, Fax (904)-644-8281, and E-mail dalal@chem.fsu.edu, or Alex I. Smirnov, 506 S. Mathews, Urbana, IL 61801, Tel. (217)-244-2252, Fax (217)-333-8868, and E-mail asmrnv@ierc.scs.uiuc.edu.

† Florida State University.

‡ College of Medicine, University of Illinois.

§ College of Veterinary Medicine, University of Illinois.

⊥ Department of Chemistry, University of Illinois.

|| University of Florida.

⊗ Abstract published in *Advance ACS Abstracts,* November 15, 1997.

S1089-5647(97)03023-X CCC: $14.00

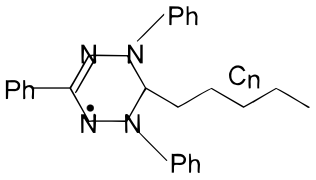

Figure 1. General structure of verdazyl radicals studied. For *n*-butyl-substituted 2,4,6-triphenylverdazyl $n = 4$.

Here we report a single-crystal EPR investigation on 3-*n*-butyl-2,4,6-triphenylverdazyl at multiple EPR frequencies from 1.4 to 94.3 GHz. The angular dependence of peak-to-peak line width and *g*-factor provide direct evidence for a pseudo-low-dimensional spin exchange for this magnetic material. The logarithmic frequency dependence of the line width at the magic angle ($\theta \approx 54.7°$) orientation of the crystal *c*-axis with respect to the magnetic field points toward a two-dimensional exchange model. The results should be of general significance to those interested in the field of organic magnetism.

Materials and Methods

Synthesis and Crystal Growth. Verdazyl radicals (1,2,3,4-tetrahydro-*s*-tetrazin-1-(2*H*-yls)) (general structure shown in Figure 1) were prepared by crown-ether-assisted solid−liquid phase-transfer catalysis, as described in detail earlier.[27] Sample purity was assessed by UV−visible absorption spectroscopy.[27] EPR spectroscopy of millimolar toluene solutions identified the synthesized compounds as verdazyl-free radicals. As an example, Figure 2 shows the EPR spectrum of *n*-butyl-substituted 2,4,6-triphenylverdazyl ($n = 4$ in Figure 1), which demonstrates the nine-line hyperfine pattern characteristic of an unpaired electron coupled to four equivalent nitrogen nuclei (nuclear spin $I = 1$). The observed spectrum is indeed typical for verdazyls.[29] Concentrations of free radicals as measured by double-integration of the EPR spectra correlated well with the amount of dissolved material, thus confirming sample authenticity and purity.

Verdazyl crystals were grown by slow evaporation of saturated solutions prepared in benzene/methylene chloride or methyl ethyl ketone. The crystals appeared under a microscope as dark green needles up to 3 mm long. It is noteworthy that we were able to obtain EPR-quality single crystals from many substituted verdazyl compounds using this method. For example, three compounds ($n = 4$, 6, and 8) from the verdazyl series described in ref 27 gave crystals of optical quality. Here we summarize our EPR results for the $n = 4$ (i.e., *n*-butyl) compound.

A single crystal of 3-*n*-butyl-2,4,6-triphenylverdazyl (approximately $0.5 \times 0.1 \times 0.1$ mm^3) was selected under the microscope and fixed inside a quartz capillary (i.d. = 0.7 mm, o.d. = 0.87 mm, length = 10 cm, VitroCom, Inc., Mountain Lakes, NJ) in such a way that the long axis of the crystal was perpendicular to the capillary. The same sample was used for all EPR measurements at multiple frequencies from 1.4 to 94.3 GHz.

EPR Measurements. X-band (8.8-9.5 GHz) and E-115Q Q-band (34.4−35.5 GHz) EPR experiments were carried out with Varian (Palo Alto, CA) Century Series E-112 and Varian E-115Q EPR spectrometers, respectively. The sample temperature was varied from 4.2 to 300 K with an Air Products (Allentown, PA) variable-temperature cryostat. The magnetic field in these experiments was calibrated by a tracking NMR Gaussmeter (Varian Model 92980102P). The microwave frequency was measured by a Hewlett Packard frequency divider (Model 5260A), a Fluke (Everett, WA) multicounter (Model 1910A), and an EIP-578 in-line microwave frequency counter (EIP Microwave, Inc., San Jose, CA).

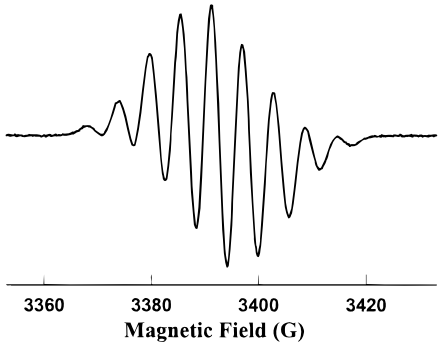

Figure 2. X-band (9.5 GHz) EPR spectrum from a dilute deoxygenated solution of 3-*n*-butyl-2,4,6-triphenylverdazyl ($n = 4$ in Figure 1) in toluene at room temperature. The spectrum shows hyperfine splitting (5.8 G) from four equivalent nitrogen nuclei ($I = 1$), which is typical for the verdazyl unit.

For L-band (1.4 GHz) EPR measurements we used a spectrometer[30] having a locally developed microwave bridge, a Varian E-9 console, an electromagnet (Alpha, Inc., Hayward, CA), and a loop-gap resonator (National Biomedical ESR Center, Medical College of Wisconsin, Milwaukee, WI).

For all these spectrometers, the data acquisition was carried out with an IBM personal computer with an IBM analog-digital card and a commercial EPR software package (Scientific Software Services, Bloomington, IL).

The W-band (94.0−94.5 GHz) EPR spectrometer constructed at the University of Illinois EPR Research Center has been described elsewhere.[31,32] The scan range and the center of magnetic field provided by an Oxford custom-built 7 T superconducting magnet were calibrated with a Metrolab precision NMR teslameter PT 2025 (GMW Associates, Redwood City, CA).

Positioning and orientational studies of the crystal in the magnetic field at L-, X-, and W-band EPR frequencies were carried out with homemade goniometers. The W-band goniometer for sample rotation about the axis perpendicular to the axis of superconducting solenoid was developed in collaboration with Prof. John A. Weil (University of Saskatchewan, Canada). For orientation of the crystal in the magnetic field, the long (needle) axis was set as the reference for the (*z*)-direction ($\theta = 0°$).

To improve the accuracy of line width measurements at various EPR frequencies, we used aqueous solutions of deuterated nitroxide Tempone (2,2′,6,6′-tetramethyl-4-piperidone-1-nitroxide; Cambridge Isotope Laboratories, Inc., Andover, MA). Isotropic nitrogen hyperfine splitting was measured by computer simulations,[33] which included second-order corrections, and was used to cross-calibrate the magnetic field scans.

Results and Discussion

Angular Dependence of EPR Line Width. It is well established in the literature[9,14,16,27] that in the solid phase the EPR spectra of all verdazyls exhibit only a single line of about 2−5 G peak-to-peak width, while a nine-line hyperfine pattern observed in solution (cf. Figure 2). Such EPR spectral narrowing is the result of the fast Heisenberg spin exchange between neighboring molecules.[9,14,27] All these earlier EPR studies were carried out with powder or microcrystalline samples. More detailed information on the anisotropy of the spin−spin interaction can be obtained in a single-crystal EPR experiment, as discussed below.

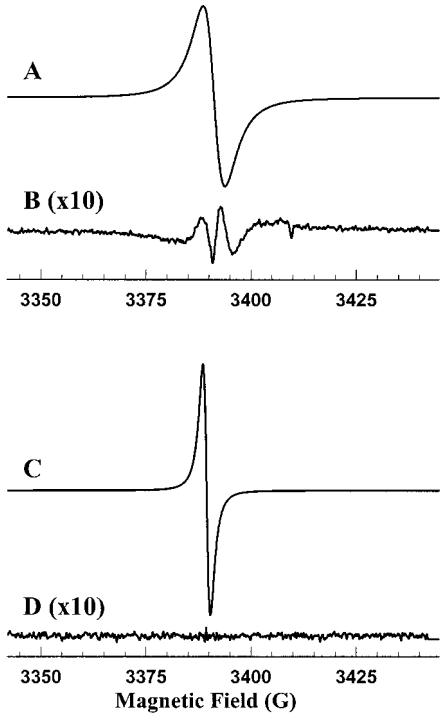

Figure 3. X-band (9.5 GHz) EPR spectra from a single crystal of 3-*n*-butyl-2,4,6-triphenylverdazyl at room temperature and the results of least-squares best fits to a Lorentzian function. Top: Orientation of the crystal in a magnetic field corresponding to $\theta = 0°$. Although the experimental spectrum (A) is close the Lorentzian line shape, the residual, a difference between the experiment and the fit, shown in 10-fold amplification (B), reveals some deviations of the experimental section from the fit. Bottom: Orientation of the crystal in a magnetic field corresponding to the "magic angle" orientation ($3\cos^2(\theta) - 1 = 0$; $\theta \approx 54.7°$). The fit of the experimental spectrum (C) to the Lorentzian line shape is excellent. Residual (D), shown in 10-fold amplification, reveals only random noise.

For a low-dimensional magnetic sample the spin Hamiltonian can be written in a general form as

$$H = Z + E + D \tag{2}$$

where Z is the Zeeman, E is the spin exchange, and D is the dipolar term, the latter being the sum of secular, D_0, and nonsecular, $D_{\pm1}$ and $D_{\pm2}$, terms. For the magnetic chains of a low-dimensional material the secular term D_0 is proportional to $(1 - 3\cos^2\theta)$, while $D_{\pm1}$ and $D_{\pm2}$ are proportional to $(\sin\theta\cos\theta)$ and $\sin^2\theta$, respectively.[21] This specific dependence of the dipolar term upon the crystal orientation allows one to separate the secular and nonsecular terms by orienting the crystal in the magnetic field with respect to the *c*-axis; at $\theta = 0°$ the nonsecular terms vanish, while at $(1 - 3\cos^2\theta) = 0$ (magic angle), the secular term D_0 goes to zero and only nonsecular terms are retained, causing specific changes in the shape of the EPR spectrum.

Figure 3 shows experimental room-temperature X-band EPR spectra from the 3-*n*-butyl-2,4,6-triphenylverdazyl crystal at $\theta = 0°$ (A) and $\theta \approx 54.7°$ (C) orientations. Both spectra were least-squares-simulated with Lorentzian functions by means of a previously described computer program.[33] Differences between the experimental and the simulated spectra are shown in 10-fold amplification as B and D, respectively (Figure 3). It is clear that at $\theta = 0°$ (Figure 3A,B) the spectrum cannot be fitted with a Lorentzian function satisfactorily, while at $\theta \approx 54.7°$ (Figure 3C,D) the fit is good. This is in agreement with other EPR studies of low-dimensional magnetic systems which have established a Lorentzian line shape for the magic angle orientation and a non-Lorentzian line shape for $\theta = 0°$.[12,21,26,28]

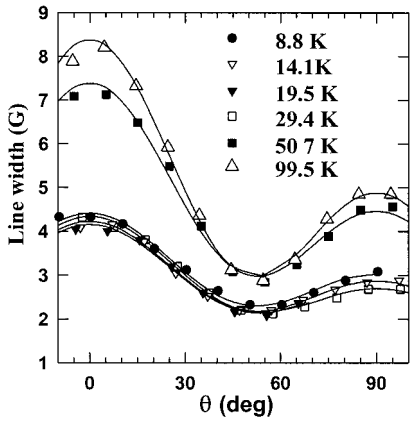

Figure 4. Peak-to-peak X-band (9.5 GHz) EPR line width at various temperatures. Lines correspond to the best least-squares fit of the experimental data to the theoretical dependence given by eq 1 with $n = 2$ and the addition of nonsecular terms.[22]

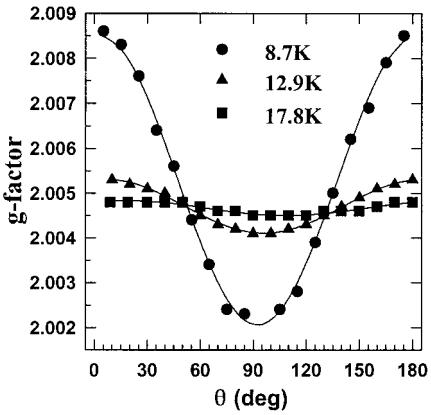

Figure 5. Angular variation of the *g*-factor at 8.7, 12.9, and 17.8 K measured from X-band (9.5 GHz) EPR data. Note, that there is no *g*-shift at the magic angle crystal orientation in the magnetic field.

More definite evidence for the low dimensionality of the spin diffusion in this crystal was provided by the anisotropic behavior observed for the peak-to-peak EPR line width. Figure 4 shows the peak-to-peak EPR line width measured at the X-band for the same crystal at various temperatures. Lines correspond to the best least-squares fit of the experimental data to the theoretical dependence given by eq 1 with $n = 2$ and the addition of nonsecular terms.[22] This shape of angular dependence of the peak-to-peak EPR line width is characteristic for low-dimensional systems. The data in Figure 4 strongly suggest that the paramagnetism of this verdazyl crystal can be described as a low-dimensional Heisenberg spin system over a wide temperature range.

Angular Dependence of *g*-Factor. The anisotropy of resonance conditions for verdazyls has been noted in other EPR studies based on the observation of the EPR signal for powder samples,[34] which yields the sum of spectra over all microcrystalline orientations. Results of experiments with single crystals we present here provide an insight for the origin of the *g*-anisotropy in verdazyls. Figure 5 shows angular dependence of the *g*-factor measured at three different temperatures at the X-band. For the crystal, the shift of the resonance position ΔB results from "classical" or dipolar, ΔB_{dip}, and dynamical or spin exchange, ΔB_{ex}, contributions:[26]

$$\Delta B = \Delta B_{dip} + \Delta B_{ex} \tag{3}$$

where ΔB_{dip} comes from the mean dipolar field:

$$\Delta B_{\mathrm{dip}} = \langle \mu_z \rangle \sum_{i,j} (3 \cos^2 \theta - 1) r_{ij}^{-3} \tag{4}$$

and μ_z is an average magnetic moment,

$$\langle \mu_z \rangle = \frac{\gamma^2 \hbar^2 S(S+1) B_0}{3\, k_{\mathrm{B}} (T + J)} \tag{5}$$

For magnetic chains, all vectors r_{ij} connecting two electron spins have the same direction and the dipolar shift becomes proportional to $(3 \cos^2 \theta - 1)$. If the magnitude of the dynamic shift ΔB_{ex} caused by spin exchange can be neglected compared with ΔB_{dip}, then the *g*-shift also becomes proportional to $(3 \cos^2 \theta - 1)$. Because the *g*-shift vanishes at the magic angle, the *g*-factor at this orientation should be temperature independent, as is consistent with Figure 5, wherein all three curves intersect at $\theta \approx 54°$. This and a close fit to $\cos^2 \theta$ dependence indicate that the anisotropy and temperature dependence of the dynamical shift ΔB_{ex} combined with other effects (e.g., surface demagnetizing fields which are difficult to account for because of the irregular shape of the crystal) can be indeed neglected.

Temperature Dependence of EPR Line Width and *g*-Factor. The temperature dependence of EPR peak-to-peak line width for several angles and temperatures is shown in Figure 4 and summarized in Figure 6 for the magic angle crystal orientation. The line width behavior closely follows the theoretical predictions[26] for a two-dimensional spin system: with decreasing temperature, the line width approaches a broad minimum (at around 16 K for this system) before rising sharply as the system approaches the antiferromagnetic phase transition temperature.

Figure 7 shows temperature dependence of the *g*-factor along the $\theta = 0°$ (parallel), $\theta = 90°$, and $\theta \approx 54.7°$ crystal orientations in the magnetic field. The *g*-factor for the magic angle orientation (open circles, Figure 7) remains constant within experimental accuracy over a broad temperature range, as follows from eq 4, while $g_{\|}$ and $g_{\perp}$ diverge as the system approaches T_c from above. The observed effect is in agreement with studies of the temperature effect on the shift of the resonance field for other low-dimensional magnetic materials.[22,25] For example, for a linear-chain antiferromagnet it has been shown that:[25]

$$\hbar\omega_{\|} = g_{\|}\mu_B B + 2A \tag{6}$$

$$\hbar\omega_{\perp} = g_{\perp}\mu_B B - A$$

where

$$A = g\mu_B B \frac{3\alpha}{5x}\left(\frac{2 + ux}{1 - u^2} - \frac{2}{3x}\right) \tag{7}$$

$$\alpha = -\frac{g^2 \mu_B^2}{2Ja^3}, \quad K = \frac{2JS(S+1)}{kT}$$

$$u = \coth K - \frac{1}{K}, \quad x = \frac{1}{K}$$

and *a* is the nearest neighbor distance along the chain.

As follows from eq 6, the *g*-shifts for the parallel and perpendicular orientations should have opposite signs and have a 2-fold difference in magnitude; this is indeed in agreement with the experimental data shown in Figure 7.

Frequency Dependence of Magic Angle EPR Line Width. The frequency dependence of the EPR line width offers another opportunity to test the dimensionality of the spin system. Figure 8 shows the angular dependence of the peak-to-peak EPR line width measured at room temperature at 1.4, 9.5, and 94.3 GHz for the same verdazyl crystal. At all these EPR frequencies the line width anisotropy has the form that is characteristic for a low-dimensional system, although at the L-band (1.4 GHz) contributions from nonsecular terms are smaller and $(3 \cos^2 \theta - 1)$ dependence is less noticeable than at higher frequencies. At the magic angle orientation of the crystal in a magnetic field, the shape of the EPR spectra at L-, X-, Q-, and W-band was fitted well by a Lorentzian function. Figure 9 shows that between 1.4 and 35 GHz the line width decreases linearly, with the logarithm of the resonance frequency ω following an

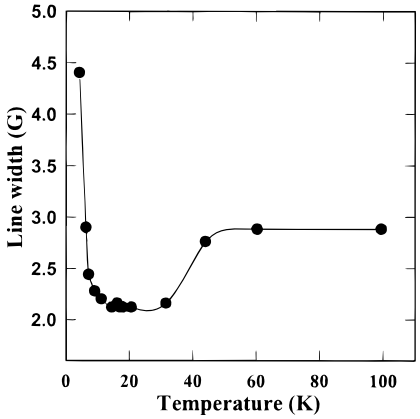

Figure 6. Temperature dependence of the X-band (9.5 GHz) EPR peak-to-peak line for the magic angle ($\theta \approx 54.7°$) crystal orientation in the magnetic field.

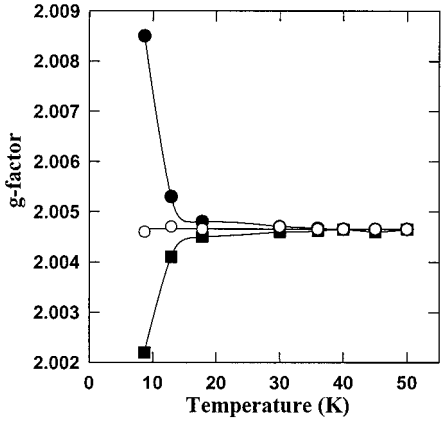

Figure 7. Temperature dependence of the *g*-factor along the $\theta = 0°$ (parallel; ●), $\theta = 90°$ (perpendicular; ■), and magic angle $\theta \approx 54.7°$ (○) crystal orientations in the magnetic field.

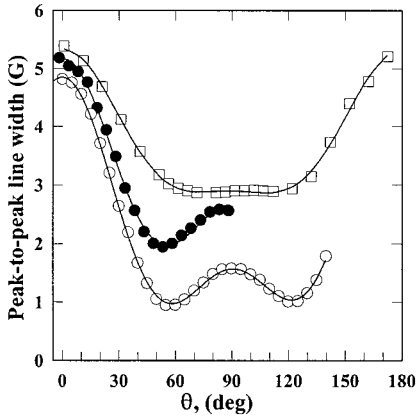

Figure 8. Angular dependence of the experimental peak-to-peak EPR line width measured at room temperature at 1.4 GHz (L-band, □), 9.5 GHz (X-band, ●), and 94.3 GHz (W-band, ○).

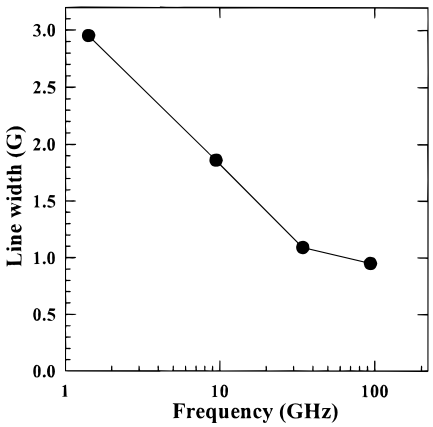

Figure 9. Magic angle ($\theta \approx 54.7°$) peak-to-peak EPR line width measured at room temperature over approximately two decades of frequency using four different EPR spectrometers. Lines correspond to the best least-squares fit of experimental data to the theoretical dependence given by eq 1 with $n = 2$ and the addition of nonsecular terms.[22]

established dependence for two-dimensional systems:[21,35]

$$\Delta B_{p-p} = \text{const} - A\frac{\omega_d^2}{D}\ln \omega \qquad (8)$$

where A is a coefficient that depends on the two-dimensional lattice, ω_d is the dipolar frequency, and D is the spin diffusion coefficient. A breakdown of this weak logarithmic dependence at 94.3 GHz is possibly associated with breaking of the spin-exchange conditions between the parts of the crystal (i.e., imperfections in the crystal structure) or effects of surface demagnetization on the narrow (<1 G) line. Inhomogeneities of the magnetic field supplied by a superconducting magnet appear not to be the reason for the observed deviation from ln ω dependence; based on measurements of deuterated nitroxide solution, this inhomogeneity over the sample region can be estimated as less than 30 mG, i.e. within the specified 1 ppm value. Perhaps EPR studies even at higher EPR frequencies can shed light on the origin of the deviation of the magic angle line width from the ln ω dependence.

Narrowing of the magic angle EPR line width with the resonance frequency also occurs for one-dimensional spin systems.[28,36] This narrowing can be well described by the Kubo−Tomita theory.[29] The theory predicts a $\omega^{-1/2}$ dependence upon resonance frequency, which was indeed experimentally observed for one-dimensional systems.[28,36] Although we have measured line widths only at four frequencies, our data fit better to a ln ω dependence than to a $\omega^{-1/2}$, pointing toward a two-dimensional spin model.

Conclusions

In conclusion, this study demonstrates several points. First, it is easy to grow single crystals of many C-5-substituted verdazyls by the slow evaporation of their saturated solutions in benzene/methylene chloride. The crystals grow usually as long dark green needles and show little or no tendency to twinning, as evidenced by the lack of site splitting in the EPR spectra. Second, single-crystal multifrequency EPR, especially as a function of temperature and crystal orientation, can serve as a sensitive probe for studying spin dynamics in low-dimensional spin systems. Third, we have shown that the *tert*-butyl-substituted verdazyl serves as a good model for a low-dimensional spin system. Fourth, the EPR theory of low-dimensional systems which was applied earlier, primarily to inorganic metal complexes, has been found to hold good also for the current study on an organic compound. The authors hope that this report will stimulate further theoretical and experimental investigations of verdazyls as materials with novel magnetic properties.

Acknowledgment. This work used the resources of the Illinois EPR Research Center (NIH P-41-RR01811). A.K. and S.B. thank the U.S. Army Research Office (Contract DAAL03-92-G-0195) for support. N.D. thanks the Florida State University for financial support. This publication was also supported by a postdoctoral fellowship, grant number 1 F32 CA 73156 (T.I.S.), from the National Cancer Institute. Its contents are solely the responsibility of the authors and do not necessarily represent the official views of the National Cancer Institute.

References and Notes

(1) *Proceedings of the Symposium on the Chemistry and Physics of Molecular Based Magnetic Materials*, The Chemical Society of Japan Meeting. Oct. 25−30, 1992, Tokyo, Japan.
(2) Iwamura, H., Miller, J. S., Eds. *Mol. Cryst. Liq. Cryst.* **1992**, *232*−*233*, 1−728.
(3) Jacobs, S. A.; Schultz, D. A.; Jain, R.; Novak, J.; Dougherty, D. A. *J. Am. Chem. Soc.* **1993**, *115*, 1744.
(4) Platz, M. S. *Org. Photochem.* **1991**, *11*, 367.
(5) Rassat, A. *Pure Appl. Chem.* **1990**, *62*, 223.
(6) Buchachenko, A. I. *Russ. Chem. Rev.* (Engl. Transl.) **1990**, *59*, 307.
(7) Allemand, P.-M.; Srdanov, G.; Wudl, F. *Synth. Met.* **1991**, *41*, 3245.
(8) Yamaguchi, K.; Toyoda, Y.; Nakano, M.; Takayuki F. *Synth. Met.* **1987**, *19*, 87.
(9) Dormann, E.; Winter, H.; Gotschy, B.; Naarmann, H. *Phys. Scr.* **1993**, *T49*, 731.
(10) Mukai, K.; Wada, N.; Jamali, J. B.; Achiwa, N.; Narumi, Y.; Kindo, K.; Kobayashi, T.; Amaya, K. *Chem. Phys. Lett.* **1996**, *257*, 538.
(11) Mukai, K.; Nedachi, K.; Takiguchi, M.; Kobayashi, T.; Amaya, K. *Chem. Phys. Lett.* **1995**, *238*, 61.
(12) Mukai, K.; Kawasaki, S.; Jamali, J. B.; Achiwa, N. *Chem. Phys. Lett.* **1995**, *241*, 618.
(13) Mukai, K.; Konishi, K.; Nedachi, K.; Takeda, K. *J. Phys. Chem.* **1996**, *100*, 9658.
(14) Pilawa, B. *J. Magn. Magn. Mater.* **1995**, *140*−*144*, 1653.
(15) Agawa, K.; Okuno, T.; Yamaguchi, K.; Hasegawa, M.; Inabe, T.; Maruyama, Y.; Wada, N. *Phys. Rev. B* **1994**, *46*, 3975.
(16) Winter, E. D.; Dyakonow, W.; Gotschy, B.; Naarmann, A. L; Walker, N. *Ber. Bunsen-Ges. Phys. Chem.* **1992**, *96*, 922.
(17) Mukai, K.; Nedachi, K.; Jamali, J. B.; Achiwa, N. *Chem. Phys. Lett.* **1993**, *214*, 559.
(18) Azuma, N.; Yamauchi, J.; Mukai, K.; Ohya-Nishiguchi, H.; Deguchi, Y. *Bull. Chem. Soc. Jpn.* **1973**, *46*, 2728.
(19) Bonner, J. C.; Fisher, M. E. *Phys. Rev.* **1964**, *A135*, 640.
(20) Bencini, A.; Gatteshi, D. *Electron Paramagnetic Resonance of Exchange Coupled Systems*; Springer-Verlag: Berlin, 1990; p 287.
(21) *Magnetic Properties of Layered Transition Metal Compounds*, L. J. De Jongh, Ed.; Kluwer Academic Publishers: Dordrecht, Netherlands, 1990; p 419.
(22) Turek, P. *Mol. Cryst. Liq. Cryst.* **1991**, *233*, 191.
(23) Benner, H. *Phys. Lett.* **1979**, *70A*, 225.
(24) Samanta, R.; Pal, A. K. *J. Phys. Chem. Solids* **1996**, *57*, 1791.
(25) Nagata, K.; Tazuke, Y. *J. Phys. Soc. Jpn.* **1972**, *32*, 337.
(26) Richards, P. M.; Salomon, M. B. *Phys. Rev.* **1974**, *B9*, 32.
(27) Dietz, R. E.; Merritt, F. R.; Dingle, R.; Hone, D.; Silbernagel, B. G.; Richards, P. M. *Phys. Rev. Lett.* **1971**, *26*, 1186.
(28) Kubo, R.; Tomita, K. *J. Phys. Soc. Jpn.* **1954**, *9*, 888.
(29) Katritzky, A. R.; Belyakov, S. A.; Durst, H. D.; Xu, R.; Dalal, N. S. *Can. J. Chem.* **1994**, *72*, 1849.
(30) Nilges, M. J.; Waltczak, T.; Swartz, H. M. *Phys. Med.* **1989**, *5*, 195.
(31) Wang, W.; Belford, R. L.; Clarkson, R. B.; Davis, R. B.; Forrer, R. B.; Nilges, M. J.; Timken, M. D.; Watczak, T.; Thurnauer, M. C.; Norris, J. R.; Morris, A. L.; Zwang, Y. *Appl. Magn. Reson.* **1994**, *6*, 195.
(32) Smirnova, T. I.; Smirnov, A. I.; Clarkson, R. B.; Belford, R. L.; Kotake, Y.; Janzen, E. G. J. *Phys. Chem. B* **1997**, *101*, 3877.
(33) Smirnov, A. I.; Belford, R. L. J. *Magn. Reson. A* **1995**, *98*, 65.
(34) Dormann, E.; Winter, H.; Dyakonow, W.; Gotschy, B.; Lang, A.; Naarmann, H.; Walker, N. *Ber. Bunsen-Ges. Phys. Chem.* **1992**, *96*, 922.
(35) Benner, H. *J. Magn. Magn. Mater.* **1980**, *15*−*18*, 727.
(36) Lagendijk, A.; Siegel, E. *Solid State Commun.* **1976**, *20*, 709.